Infocommunications and Radio Technologies, vol. 1, no. 1, pp. 29–47, 2018.
Инфокоммуникационные и радиоэлектронные технологии. 2018. Т. 1, № 1. С. 29—47.
ISSN: 2587-9936 print / 0000-0000 online
DOI: 10.15826/icrt.2018.01.1.03

Signal and noise parameters of autodynes with the soft impedance characteristic of the active element (review)

V. Ya. Noskov [1], K. A. Ignatkov [1], D. Ya. Mishin [1],
S. M. Smolskiy [1,2], and A. P. Chupahin [1]
[1] *Institute of Radioelectronics and Information Technologies,*
Ural Federal University n. a. first President of Russia B. N. Yeltsin
32, Mira Str., Yekaterinburg, 610002, Russian Federation
[2] *Moscow Power Engineering Institute (National Research University)*
14, Krasnokazarmennaya Str., Moscow, 111250, Russian Federation
noskov@oko-ek.ru

Received on July 26, 2016

Abstract: *The general expressions for an analysis of signal and fluctuation parameters and characteristics of an autodyne oscillator are obtained, which is under an influence of the proper reflected emission from a radar object. The oscillator model represented by a parallel connection of an oscillating system and an active element with the soft impedance characteristics, also takes into consideration the internal noises of the active element. The analysis results are presented for dependences of autodyne mentioned parameters and characteristics versus the oscillator operation mode and a value of the "softness" index of its impedance characteristics of the active element. Investigation results are necessary for engineering calculation of parameters and characteristics of the autodyne on the Gunn diode and other active elements base.*

Keywords: *autodyne, autodyne response, noisy parameters, signal parameters, oscillator operation modes.*

For citation (IEEE): V. Ya. Noskov, K. A. Ignatkov, D. Ya. Mishin, S. M. Smolskiy, and A. P. Chupahin, "Signal and noise parameters of autodynes with the soft impedance characteristic of the active element (review)," *Infocommunications and Radio Technologies,* vol. 1, no. 1, pp. 29–47, 2018. doi: 10.15826/icrt.2018.01.1.03

Сигнальные и шумовые параметры автодинов с мягкой импедансной характеристикой активного элемента (обзор) [1]

[1] Носков В. Я., [1] Игнатков К. А., [1] Мишин Д. Я.,
[1,2] Смольский С. М., [1] Чупахин А. П.

Институт радиоэлектроники и информационных технологий — РТФ,
Уральский федеральный университет
им. первого Президента России Б. Н. Ельцина
ул. Мира, 32, г. Екатеринбург, 620002, Российская Федерация
[2]*Московский энергетический институт (национальный исследовательский ун-т)*
ул. Красноказарменная, 14, Москва, 111250, Российская Федерация
noskov@oko-ek.ru

Статья поступила 26 июля 2016 г.

Аннотация: *Получены общие соотношения для анализа сигнальных и флуктуационных параметров и характеристик автодинного генератора, находящегося под воздействием собственного отражённого излучения от объекта локации. Модель генератора, представленная параллельным соединением проводимостей колебательной системы и активного элемента с мягкой импедансной характеристикой, учитывает также внутренние шумы активного элемента. Представлены результаты анализа зависимости указанных параметров и характеристик автодинов от режима работы генератора и от величины показателя «мягкости» импедансной характеристики активного элемента. Результаты исследований востребованы для инженерного расчёта параметров и характеристик автодинного генератора на основе диода Ганна и других активных элементов.*

Ключевые слова: *автодин, автодинный отклик, шумовые параметры, сигнальные параметры, режимы работы генератора.*

Для цитирования (ГОСТ 7.0.5—2008): Сигнальные и шумовые параметры автодинов с мягкой импедансной характеристикой активного элемента (обзор) / Носков В. Я., Игнатков К. А., Мишин Д. Я., Смольский С. М., Чупахин А. П. // Инфокоммуникационные и радиоэлектронные технологии. 2018. Т. 1, № 1. С. 29—47.

Для цитирования (ГОСТ 7.0.11—2011): Сигнальные и шумовые параметры автодинов с мягкой импедансной характеристикой активного элемента (обзор) / В. Я. Носков, К. А. Игнатков, Д. Я. Мишин, С. М. Смольский, А. П. Чупахин // Инфокоммуникационные и радиоэлектронные технологии. — 2018. — Т. 1, № 1. — С. 29—47.

[1] Статья является обзорной версией ряда докладов автодинной тематики, представленных на 25-й Международной Крымской конференции «СВЧ-техника и телекоммуникационные технологии» — КрыМиКо’2014 (Севастополь, 6—12 сент. 2015 г.).

1. Introduction

Autodynes [2] are the simplest multi-functional transceiver devices made on the base of oscillators, which simultaneously perform function of an transmitter of the probe emission and a receiver of signals reflected from the radar object or from an outside information source. As a result of nonlinear transform of microwave signals, so-called "autodyne" effect occurs in the autodyne, which leads to an autodyne response (the autodyne useful signal). Extraction of the autodyne response in the form of low-frequency useful signal on the external microwave influence and its processing enables a possibility to find out the needed information about the reflecting object or about a transmitted message. With the help of autodyne devices, one can solve a wide circle of problems in the radar technology, communications, and measuring techniques in various applications [1–7].

A great number of publications in the form of reviews, scientific and engineering papers and books (see reference list in [7]) is devoted to researches of signal formation peculiarities, studying of autodyne noise parameters and characteristics. Nevertheless, in known publications, the influence on various parameters and characteristics of the autodyne oscillation mode and on a type of the impedance characteristic of its active element (AE) were not considered at all. Here, under impedance characteristics we understand a dependence of the averaged AE conductivity over oscillation period versus the oscillation amplitude and other factors. Results of these researches are necessary for a correct choice of the coupling coefficient between the oscillator and a load, a type of AE characteristic and a position of the operation point on the volt-ampere curve of AE for which the best conditions may be ensured to reach the required parameters and characteristics of the oscillator as an *autodyne*.

The goal of this paper is to perform a research for dependence of output power, transfer, signal and noise parameters, as well as the processing speed upon the chosen steady-state oscillation mode for the microwave and millimeter-wave autodyne oscillator. Results of such an analysis were discussed in our previous publications [8–11].

2. Parameters of stationary mode

Main parameters, which characterize the steady-state operation mode of microwave and millimeter-wave oscillators, in the vicinity of which the autodyne effect is demonstrated, are the output power P_{ex}, an amplitude A and a fre-

[2] In the world English-language literature, together with the widespread term "autodyne", one may often use the terms "oscillator-detector", "self-oscillating mixer" (SOM), "self-mixing oscillator", "self-detecting oscillator" etc.

quency ω of high-frequency oscillations. To obtain these parameters, we consider the simplest single-circuit oscillator model in the form of parallel connection of resonator (cavity) conductivity Y_c and the resistive load G_L, and the "electronic" AE conductivity Y_e averaged over the oscillation period.

The expression for total conductivity Y_c of the high-Q cavity in the vicinity of its natural frequency ω_c is given by: $Y_c = G_c[1 + j2Q_c(\omega - \omega_c)/\omega_c]$, where G_c and Q_c are the active conductivity of cavity losses and its own Q-factor, accordingly. At that, we assume that approximation of the electronic conductivity averaged over the period $Y_e(A,\omega) = G_e + jB_e$, which depends on oscillation amplitude and frequency, has the following form [8, 12]:

$$Y_e(A,\omega) = -G_{e0}[1-(A/A_{\max})^n + \nu_g(\omega-\omega_0)/\omega_0] - \\ -jB_{e0}[1-\nu_b(A-A_0)/A_0], \quad (1)$$

where G_{e0} is the resistive AE conductivity when oscillations are absent; $A_{\max}$ is oscillation amplitude on AE, at which the G_e conductivity becomes equal to zero; n is the "softness" index of the AE impedance characteristic; A_0, ω_0 are steady-state amplitude A and frequency ω of the autonomous oscillator; B_{e0} is the AE reactive conductivity for $A = A_0$; ν_g, ν_b are coefficients defining a sensitivity of appropriate AE conductivities with respect to variations of amplitude A and frequency ω at small offset from the fundamental frequency.

Then, from the conductivity balance condition with account of (1) and the load G_L, we obtain two real steady-state mode equations, from which we determine two unknown quantities for this problem: the frequency ω_0 and the relative amplitude $u_{r.a} = A_0 / A_{max}$ of steady-state autonomous oscillator values:

$$\omega_0 = \omega_c[1 + (\mathrm{tg}\Theta_0 / 2Q_L)],\ u_{r.a} = (1 - g_c - g_L)^{1/n}, \quad (2)$$

where $\Theta_0 = \mathrm{arctg}[B_{e0} / G_e(A_0, \omega_0)]$ is the phase angle of AE signal delay; Q_L is the loaded Q-factor of the oscillating system:

$$Q_L = Q_c g_c / (g_c + g_L) = Q_c g_c / (1 - u_{r.a}^n); \quad (3)$$
$$g_c = G_c / G_{e0};\ g_L = G_L / G_{e0}.$$

Calculation results according to (1) are presented in Fig. 1 in the form of plots of normalized curves' modulus of $g_e(u_{r.a}) = G_e / G_{e0}$ (*a*) and $u_{r.a}(g_L)$ (*b*), obtained provided the condition $\omega = \omega_0$ for different values of n exponent[3]. As we see from the plots in Fig. 1, when the n exponent increase, these characteristics in a more extent come away from the "soft" characteristic (for which the

[3] Here and further, if we do not specially mention otherwise, the plots are drawn for the following values of n exponent: $n = 0.5$ (curves *1*); $n = 1$ (curves *2*); $n = 2$ (curves *3*); $n = 4$ (curves *4*).

AE conductivity averaged over the period monotonically drops in modulo) and arrives to the “rigid” impedance characteristic (when AE averaged conductivity at first increases at amplitude growth, and then reduces).

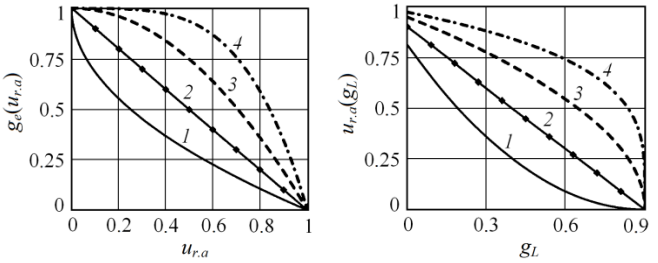

(*a*) (*b*)

Fig. 1. Plots of functions $g_e(u_{r.a})$ (*a*) and $u_{r.a}(g_L)$ (*b*).

Рис. 1. Графики зависимостей $g_e(u_{r.a})$ (*a*) и $u_{r.a}(g_L)$ (*b*)

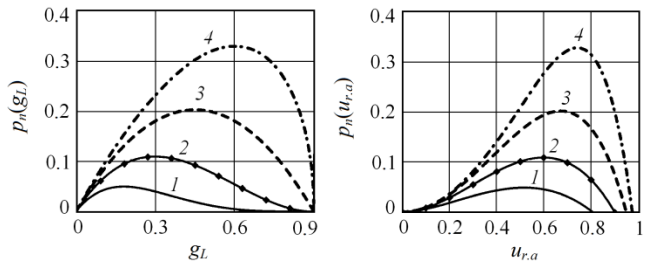

(*a*) (*b*)

Fig. 2. Plots of functions $p_n(g_L)$ (*a*) and $p_n(u_{r.a})$ (*b*).

Рис. 2. Графики зависимостей $p_n(g_L)$ (*a*) и $p_n(u_{r.a})$ (*b*)

Taking into consideration the expression (1), the equation for delivered power P_{ex}, acting on the load conductivity G_L, has a form: $P_{ex} = A_0^2 G_L / 2 = P_m p_n$. Here $P_m = A_{\max}^2 G_{e0} / 2$ is formally realizable AE maximal power; $p_n = P_{ex} / P_m$ is the normalized characteristic of the oscillator output power versus the normalized conductivities of the cavity g_c and load g_L losses:

$$p_n = g_L (1 - g_c - g_L)^{2/n} = (1 - g_c - u_{r.a}^n) u_{r.a}^2 . \qquad (4)$$

Functions’ families of the normalized output power p_n versus the normalized load conductivity g_L and the relative amplitude $u_{r.a}$ calculated in accordance with (4) for $g_c = 0.9$ and various values of n, are shown in the plots in Fig. 2.

From curves in Fig. 2 we see that at the optimal coupling oscillator-load, when $g_L = g_{L(\text{opt})}$, the power delivered to the load has the maximal value. If

$g_L > g_{L(\text{opt})}$, the power transferred to the load is more than the power dissipated in the cavity. This case refers usually as the "over-coupling" mode [13]. In the "under-coupling" mode $g_L < g_{L(\text{opt})}$ and the load power becomes less than the cavity power. The under-coupling region is on the right from the power maximum in plots of Fig. 2, where the relative AE amplitude $u_{r.a}$ is more than the amplitude, at which the power load maximum is observed: $u_{r.a} > u_{\max}$, and in over-coupling region – on the left, when $u_{r.a} < u_{\max}$.

The analysis on output power extremum of (4) with account of (2) allows formula obtaining for calculation of maximal power $P_{\max} = P_m \cdot p_{\max}$ in the load, as well as the optimal value of load conductivity $G_{L(\text{opt})} = G_{e0} g_{L(\text{opt})}$ and the relative oscillation amplitude $u_{\max}$ on AE:

$$g_{L(\text{opt})} = n(1-g_c)/(n+2), \tag{5}$$

$$u_{\max} = A_{0(\text{opt})} / A_{\max} = 2(1-g_c)^{1/n}/(n+2), \tag{6}$$

where $p_{\max}$ is the normalized characteristic of maximal output power:

$$p_{\max} = \frac{n(1-g_{\text{p}})}{(n+2)}\left[1-g_c-\frac{n(1-g_c)}{(n+2)}\right]^{2/n}. \tag{7}$$

3. Equations for autodyne parameters and characteristics

The autodyne effect in various oscillators consists in variations of oscillation parameters, which are described by linearized equations in the vicinity of the steady-state mode for relative variations of oscillation amplitude $a(\tau)$ and frequency $\chi(\tau)$ [14]:

$$a(\tau) = \Gamma K_a \cos[\delta(\tau) - \psi], \tag{8}$$

$$\chi(\tau) = -\Gamma L_a \sin[\delta(\tau) + \theta], \tag{9}$$

where Γ is the reflection coefficient reduced to the oscillator output; τ is delay time of reflected emission; K_a, L_a are coefficients of autodyne amplification and autodyne frequency deviation, relatively:

$$K_a = \eta\sqrt{1+\rho^2}\,/\,\alpha(1-\gamma\rho),\ L_a = \eta\sqrt{1+\gamma^2}\,/\,Q_L(1-\gamma\rho); \tag{10}$$

η is efficiency of the autodyne oscillation system:

$$\eta = g_L/(g_c+g_L) = (1-g_c-u_{r.a}^n)/(1-u_{r.a}^n), \tag{11}$$

$\delta(\tau)$ is a phase incursion of reflected microwave emission; $\gamma = \beta/\alpha$ and $\rho = \varepsilon/Q_L$ are coefficients of oscillator non-isochronity and non-isodromity, ac-

cordingly; $\psi = \text{arctg}(\rho)$, $\theta = \text{arctg}(\gamma)$ are phase offset angles of autodyne variations of self-oscillation amplitude and frequency [14]; α, β, ε are differential parameters [9]:

$$\alpha = n(1 - g_c - g_L)/2(g_c + g_L) = nu_{r.a}^n / 2(1 - u_{r.a}^n), \quad (12)$$

$$\beta = \nu_b \text{tg}\Theta_0 / 2(g_c + g_L) = \nu_b \text{tg}\Theta_0 / 2(1 - u_{r.a}^n), \quad (13)$$

$$\varepsilon = \nu_g / 2(g_c + g_L) = \nu_g / 2(1 - u_{r.a}^n). \quad (14)$$

4. Transfer functions of the autodyne response

Main parameters characterizing the process of reception, frequency conversion and passage of oscillator response on the influence of the radar object reflection emission are coefficients of autodyne amplification K_a, frequency deviation L_a and transfer function in power L_P. Dependence of these parameters upon the oscillator operation mode can be considered using above-obtained equations (2), (3), (11—14) for inherent parameters [9, 14].

Calculation results of functions $K_a(g_L)$, $K_a(u_{r.a})$ and $L_a(g_L)$, $L_a(u_{r.a})$ are presented in Fig. 3 in the form of the curves' family obtained for various n exponent values. Initial data for these and further calculations are accepted as follows (in conformity with the 8mm-range Gunn-diode oscillator): $g_c = 0.1$, $\nu_g = 1$, $\nu_b = 1$, $G_0 = 10$ mOhm^{-1}, $A_{\max} = 4$ V, $G_c = 1$ mOhm^{-1}, $Q_c = 200$, $\omega_0 = 2\pi \cdot 37.5 \cdot 10^9$.

From plots in Fig. 3 we see that at arriving to an excitation threshold, where the load conductivity is large and oscillations amplitude is small, the limit cycle strength α decreases, and coefficients K_a and L_a, which characterize the amplitude and frequency sensitivity to external impacts, accordingly, essentially grow. At that, autodyne amplification coefficients K_a (depending on oscillator operation mode) may be both less than 1 and exceed it significantly being tens and hundreds times.

The analysis of (10) and curves in Fig. 3 shows that the limit cycle strength α (12) is the main function depending upon an operation mode and affecting to behavior of functions $K_a(g_L)$ и $K_a(u_{r.a})$. The other components, for instance, caused by oscillator non-isochronity γ and non-isodromity ρ, introduce insignificant contribution to these functions. Application of an oscillator mode, at which the softness index has values $n > 1$, ensures the lesser benefit in coefficients K_a and L_a, than at its small values, when $n < 1$. At arriving to the mode with higher values of g_L, when oscillation amplitude is small, coefficients K_a and L_a quickly grow especially for characteristics with $n > 1$.

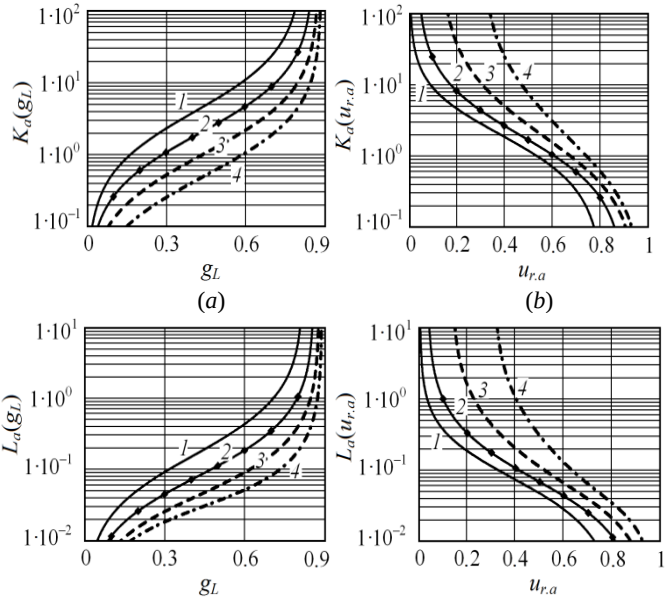

Fig. 3. Plots of functions $K_a(g_L)$ (*a*), $K_a(u_{r.a})$ (*b*) and $L_a(g_L)$ (*c*), $L_a(u_{r.a})$ (*d*).

Рис. 3. Графики зависимостей $K_a(g_L)$ (*a*), $K_a(u_{r.a})$ (*b*) и $L_a(g_L)$ (*c*), $L_a(u_{r.a})$ (*d*)

Phase offset angles ψ and θ of autodyne responses on variations of amplitude (8) and frequency (9) are auxiliary autodyne parameters. The analysis of these expressions shows that the ψ angle in the model accepted here does not depend on operation mode. It completely defines by the coefficient v_g. For phase angle θ in Fig. 4 [taking into account (13) and (14)] plots of functions $\theta(g_L)$ (*a*) and $\theta(u_{r.a})$ (*b*) are drawn at various *n*.

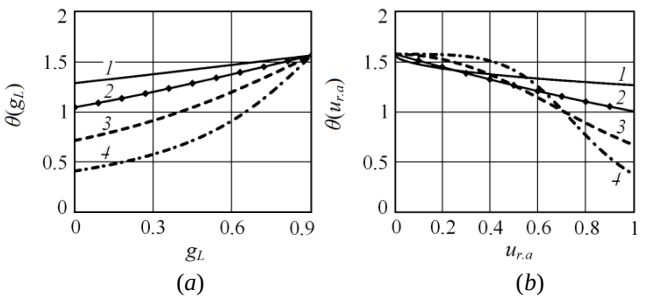

Fig. 4. Plots of functions $\theta(g_L)$ (*a*) and $\theta(u_{r.a})$ (*b*).

Рис. 4. Графики зависимостей $\theta(g_L)$ (*a*) и $\theta(u_{r.a})$ (*b*)

From plots in Fig. 4 we see that the angle θ of AFC phase offset essentially affecting on the distortion of autodyne signals in non-isochronous oscillators weakly varies at variation of the autodyne operation mode character both for small and for large values of n. This angle is mainly defined by coefficient ν_b.

Behavior of the autodyne response transfer function in power K_P has a special interest at variation of an operation mode. This function is included into expression of "power" characteristic of the autodyne (APC) describing variations of output power $\Delta P_{ex}(\tau_n)$ at variation of phase incursion of reflected emission:

$$\Delta P_{ex}(\tau_n) = P_{ex}(\tau_n) - P_{ex0} = 2\Gamma^2 K_P \cos\delta(\tau_n), \qquad (15)$$

where $P_{ex}(\tau_n)$, P_{ex0} are a current value of the load power and its value for autonomous mode; $\tau_n = \omega_0 \tau$ is normalized time. Equations for $K_P \equiv K_P(g_L)$ and $K_P \equiv K_P(u_{r.a})$ accordingly, are given by:

$$K_P = g_L(1-g_c-g_L)^{2/n}[1-2g_L/n(1-g_c-g_L)] = ,$$
$$= u_{r.a}^2(1-g_c-u_{r.a}^n)[1-2(1-g_c-u_{r.a}^n)/nu_{r.a}^n]. \qquad (16)$$

Plots of functions $K_P(g_L)$ and of the autodyne calculated, as usually, according to (16), at various n are presented in Fig. 5.

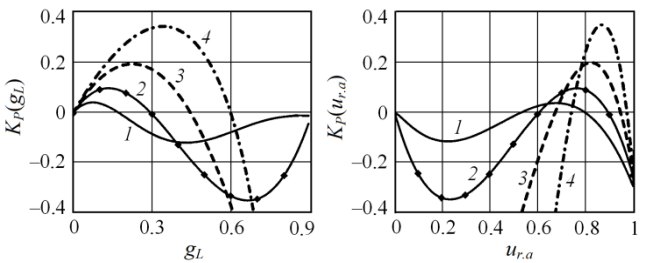

(*a*) (*b*)

Fig. 5. Plots of functions $K_P(g_L)$ (*a*) and $K_P(u_{r.a})$ (*b*).

Рис. 5. Графики зависимостей $K_P(g_L)$ (*a*) и $K_P(u_{r.a})$ (*b*)

From comparison of Figs. 2 and 5 we see that the autodyne transfer function K_P in power depends not only upon output power, which is defined also by the softness index of the impedance characteristic, but upon the oscillator-load coupling character. In the case of optimal coupling, when output power is largest, we have $K_P = 0$, and at transfer from the under-coupling mode into over-coupling and vice-versa the sign of K_P changes to the opposite. This statement represents the special interest for an adjustment procedure of the microwave oscillator to the autodyne mode.

APC calculation results $\Delta p_{ex}(\tau_n)$ at $g_c = 0.1$, $n = 4$ and $g_L < g_{L0}$ (see curve *1*) and $g_L > g_{L0}$ (see curve *2*), where g_{L0} is the conductivity at which the output power is the highest [11] are presented in Fig. 6. The frequency characteristic (AFC) calculated according (9) for the case of optimal coupling (when $g_L = g_{L0}$ is presented in Fig. 6,*b*.

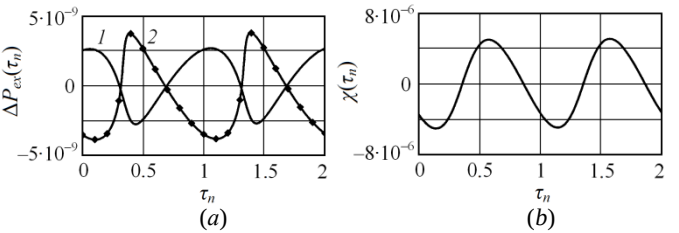

Fig. 6. Plots of APC $\Delta P_{ex}(\tau_n)$ (*a*) of the oscillator load calculated at $g_L = 0.55$ (curve *1*), and $g_L = 0.65$ (curve 2), and AFC $\chi(\tau_n)$ (*b*), obtained at $g_L = 0.6$.

Рис. 6. Графики МХА $\Delta P_{ex}(\tau_n)$ (*a*) на нагрузке генератора, рассчитанные при $g_L = 0.55$ (кривая *1*) и $g_L = 0.65$ (кривая *2*), и ЧХА $\chi(\tau_n)$ (*b*), полученная при $g_L = 0.6$

The curve *1* in Fig. 6 is obtained for the under-coupling case when the operation point on $K_P(g_L)$ (see curve *4* in Fig. 2,*a*) has the positive sign of K_P, and the curve *2* is obtained for the over-coupling case, when this sign is negative. Therefore, at transfer from the over-coupling mode into the under-coupling mode, we observe the APC inversion $\Delta p_{\text{н}}(\tau_n)$. In the optimal coupling case $g_L = 0.6$, when the output power is highest, the autodyne response is caused by frequency variations $\chi(\tau_n)$ $\chi(\tau_n)$ and amplitude $a(\tau_{\text{н}})$ only. This behavior character of APC is confirmed by experimental data presented in our review [15].

5. Operating speed parameters of autodyne oscillators

The next important autodyne parameter, which we are going to consider now, is the time constant τ_a of the autodyne response that characterizes the operation speed for response transient on the reflected emission impact, for instance, in autodyne system with emitted pulse modulation [16]: $\tau_{\text{a}} = Q_L/[\omega_0 \alpha_{11}(1-\gamma\rho)]$. At that, the boundary frequency F_{lim} (in Hz) of the autodyne response by the – 3db-level is related to the time constant τ_a by simple relation: $F_{\text{lim}} = 1/2\pi\tau_{\text{a}}$.

Calculation results for the time constant τ_a (ns) and the boundary frequency F_{lim} (GHz) in the form of functions $\tau_{\text{a}}(g_L)$, $\tau_{\text{a}}(u_{r.a})$ and $F_{\text{lim}}(g_L)$, $F_{\text{lim}}(u_{r.a})$ are presented in Fig. 7 as the curves family obtained for various *n*.

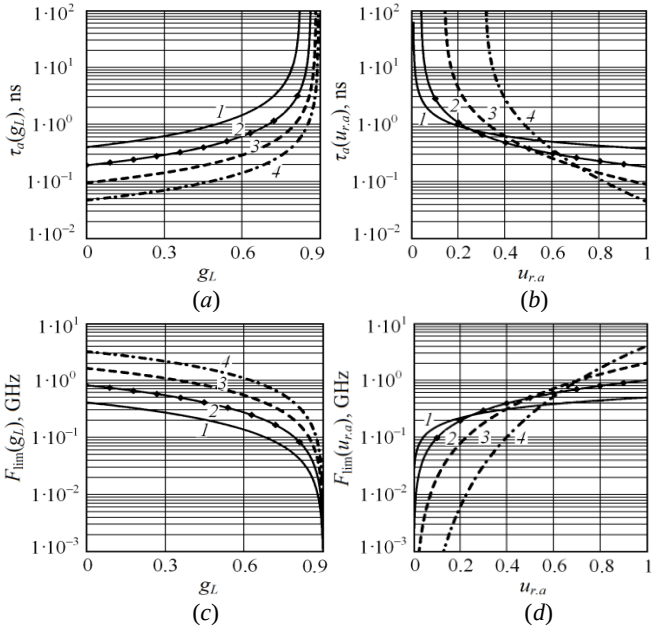

Fig. 7. Plots of functions $\tau_a(g_L)$ (*a*), $\tau_a(u_{r.a})$ (*b*) and $F_{\lim}(g_L)$ (*c*), $F_{\lim}(u_{r.a})$ (*d*).

Рис. 7. Графики зависимостей $\tau_a(g_L)$ (*a*), $\tau_a(u_{r.a})$ (*b*) и $F_{\lim}(g_L)$ (*c*), $F_{\lim}(u_{r.a})$ (*d*)

From plots of this figure, we see that at oscillator arrival to the excitation threshold, where the load conductivity is high, and amplitude is small, the time constant τ_a sharply increases, and the boundary bandwidth of quasi-harmonic signals of the autodyne response becomes essentially narrower. As we see from Fig. 7, *a* and *b*, the time constant τ_a of the 8mm-range oscillator may be located in the range from hundredth to units of nanoseconds. At that, the boundary value $F_{\lim}$ of bandwidth for output autodyne signals may be from tens of MHz to about one GHz (see curves in Figs. 7,*c* and *d*). These calculation results are well agreed with experimental data [17].

From plots obtained in Fig. 7 it also follows that utilization of the oscillator mode, at which large quantities of *n* can be realized for AE impedance characteristic softness, promotes the transient time decrease for autodyne response and, accordingly, for widening of the autodyne bandwidth.

6. Noisy parameters of the autodyne

Effective values of frequency $\Delta f_{n.ef}$ and amplitude $A_{n.ef}$ fluctuations of the oscillator used, which define the minimal level of a signal under detection,

as well as the autodyne energy potential Π, which determines the autodyne system possibilities in operation range, detection reliability for reflecting objects and in measurement accuracy of its parameters are the main autodyne noise parameters [10]. One more important feature related to noise parameters is the width of its dynamic range.

Equations for effective values of autodyne frequency $\Delta f_{n.ef}$ and amplitude $A_{n.ef}$ noises have the following view [18]:

$$\Delta f_{n.ef} = \omega_0 \sqrt{2kT_n M_n \Delta F(1+\gamma^2)/P_{ex}} \Big/ 2\pi Q_L(1-\gamma\rho), \quad (17)$$

$$A_{n.ef} = u_{r.a} A_{\max} \sqrt{2kT_n M_n \Delta F(1+\rho^2)/P_{ex}} \Big/ \alpha(1-\gamma\rho), \quad (18)$$

where $k = 1.38 \cdot 10^{-23}$ J/K is the Boltzmann constant; T_n is the equivalent noise temperature of AE; M_n is a measure of AE noise.

Formulas for calculation of an energy potential during signal registration according to frequency variation Π_F and amplitude Π_A variation can be written as [10, 18]:

$$\Pi_F = \frac{Q_L^2(1-\gamma\rho)^2 P_{ex}}{2kT_n M_n \Delta F(1+\gamma^2)}, \ \Pi_A = \frac{\alpha^2(1-\gamma\rho)^2 P_{ex}}{2kT_n M_n \Delta F(1+\rho^2)}. \quad (19)$$

The ratio of a limited value of the reflection factor $\Gamma_{\lim}$, at which the signal jumps begin, to the level of own frequency noises of the microwave oscillator, gives a value of the required dynamic range *D* of the autodyne system [19]:

$$D = \Gamma_{\lim} \sqrt{\Pi} = R / R_c, \quad (20)$$

where *R* is a threshold distance to the reflecting object expressed in emission half-wavelengths, at which levels of reflected emission and own oscillator frequency noises are equal; R_c is the same but current distance to the reflecting object. In the general form, the equation for threshold distance *R* calculation has the following view:

$$R = (1/2\pi\eta) Q_L(1-\gamma\rho)\sqrt{\Pi/(1+\gamma^2)}. \quad (21)$$

Calculation results according to (17) and (18), taking into account (3), (12) – (14) and functions $\Delta f_{n.ef}(g_L)$, $\Delta f_{n.ef}(u_{r.a})$ and $A_{n.ef}(g_L)$, $A_{n.ef}(u_{r.a})$ are presented in Fig. 8 in the form of the plot family for various *n*. The similar functions obtained as a result of calculation according to formulas (19) are shown in Fig. 9. The initial data for calculations are accepted as follows: $T_n = 300$ K; $M_n = 33$ dB; $\Delta F = 1$ kHz.

From plots in Figs. 8 and 9, we can see that curves obtained have the extreme character. At small load conductivity values g_L, where oscillation amplitude $u_{\text{отн}}$ is large enough, the oscillator provides the operation mode with minimal level of frequency $\Delta f_{n.ef}$ and amplitude $A_{n.ef}$ noises, at that, when the softness index grows, this minimum becomes lower. At that, potential extreme values coincide with minima of effective noise values.

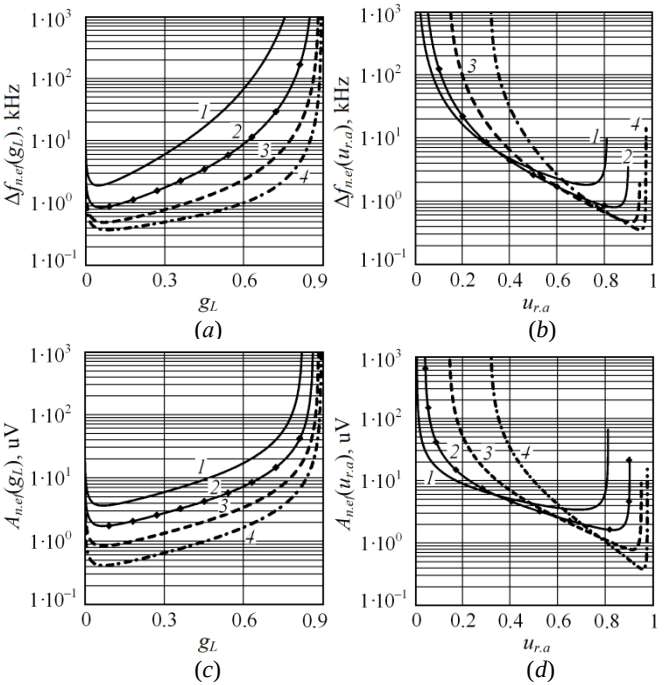

Fig. 8. . Plots of functions $\Delta f_{n.ef}(g_L)$ (*a*), $\Delta f_{n.ef}(u_{r.a})$ (*b*) and $A_{n.ef}(g_L)$ (*c*), $A_{n.ef}(u_{r.a})$ (*d*).

Рис. 8. Графики зависимостей $\Delta f_{n.ef}(g_L)$ (*a*), $\Delta f_{n.ef}(u_{r.a})$ (*b*) и $A_{n.ef}(g_L)$ (*c*), $A_{n.ef}(u_{r.a})$ (*d*)

From comparison of relative amplitude $u_{\text{отн}}(g_L)$ and output power $p_n(g_L)$, plots presented in Fig. 1,*b* and Fig. 2, with plots of effective values of frequency $\Delta f_{n.ef}(g_L)$ and amplitude $A_{n.ef}(g_L)$ noise we can see that noise minima and, accordingly, maxima of the limited energy potential $\Pi_F(g_L)$ and $\Pi_A(g_L)$ are ensured at small values of the load conductivity g_L. Additional conclusion from results obtained consists in the fact that with softness index *n* growth, the potential maximum can be achieved at large values of relative amplitude and, at increase of this index, the energy potential also grows.

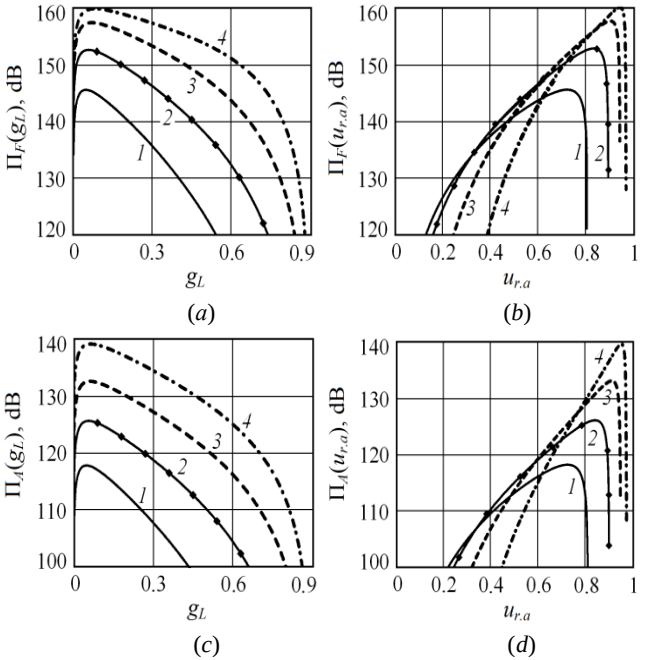

Fig. 9. Plots of functions $\Pi_F(g_L)$ (*a*), $\Pi_F(u_{r.a})$ (*b*) and $\Pi_A(g_L)$ (*c*), $\Pi_A(u_{r.a})$ (*d*).

Рис. 9. Графики зависимостей $\Pi_F(g_L)$ (*a*), $\Pi_F(u_{r.a})$ (*b*) и $\Pi_A(g_L)$ (*c*), $\Pi_A(u_{r.a})$ (*d*)

Under mentioned conditions, the oscillation amplitude u_{rel} near its maximal values $A_{\max}$, is ensured, and the output power P_{ex} is several times lesser than the largest power, which occurs at optimal coupling with the load $g_L = g_{L(\text{opt})}$. From investigations performed (see plots in Figs. 8 and 9) it follows one more result, which confirms conclusions from our publication [19], and consists in the fact that, at signal registration according to frequency variation, the higher value (by 20—30 dB) of the autodyne potential than at registration of amplitude variations.

From calculation results, at other values of relative conductivity g_c it follows that application of the high Q-factor Q_c promotes obtaining of low fluctuation level, which makes agree with known conclusions of the oscillator noise theory. In addition, at that, we obtain high values of the autodyne limited energy potential both at signal registration according to frequency variation Π_F and to the oscillation amplitude Π_A.

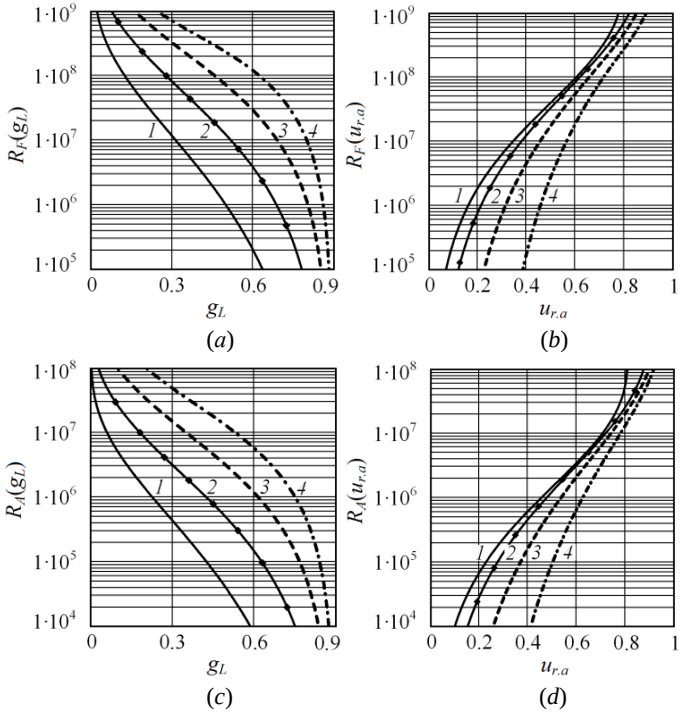

Fig. 10. Plots of functions $R_F(g_L)$ (*a*), $R_F(u_{r.a})$ (*b*) and $R_A(g_L)$ (*c*), $R_A(u_{r.a})$ (*d*).

Рис. 10. Графики зависимостей $R_F(g_L)$ (*a*), $R_F(u_{r.a})$ (*b*) и $R_A(g_L)$ (*c*), $R_A(u_{r.a})$ (*d*)

Plots of functions $R(g_L)$ and $R(u_{r.a})$ of the maximal distances to the reflecting object expressed in a number of half-wavelengths are presented[4] in Fig. 10. Calculations for these plots were performed in accordance with (21) taking into account (3) and (12) – (14), (19). From plots obtained and from curves in Fig. 9, we see that regions of oscillation parameters, where the autodyne potential is maximal, corresponds also to the region, where the system dynamic range is the highest. At that, dynamic range growth in this region relates not only to a noise level minimum, but relates with decrease of autodyne frequency deviation (see Figs. 3,*c* and *d*).

Experimental investigations data presented in [15, 20] on an example of autodyne oscillators on Gunn diodes and IMPATT diodes, qualitatively confirm the above-mentioned theoretical results.

[4] Indices *F* and *A* at *R* on plots in Fig. 10 mean belonging of this function to determination of the dynamic range at registration according to variations of frequency and amplitude, relatively.

7. Conclusions

Dependence of main autodyne parameters is analyzed on the base of the earlier-developed model such as an output power, transfer functions, an energy potential, and a dynamic range as well as noisy parameters and operation speed parameters upon the AE oscillation mode and a type of its impedance characteristic.

Investigations performed show that at choice of a type and AE operation mode for autodyne oscillator ensuring the largest value of the system energy potential, it is necessary to be guided by the following recommendations. To apply an AE type and the operation point position such that ensure the type of AE impedance characteristic, which is as close as possible to the rigid type. At that, it is necessary to set the mode of weak coupling between the oscillator and the load, ensuring the relative high values of AE oscillation amplitude, when the output power several times less than a power, which is delivered by this oscillator to the load at optimal coupling. The oscillating system must guarantee as far as possible high values of the proper Q-factor, and AE – the least value of noise measure. At that, it is necessary to note that the mode of the best energy potential differs from the mode of optimal coupling in power as well as the maximal transfer function of the autodyne response.

It is shown that in the case of autodyne signal registration in power according to an oscillator load variation from the under-coupling mode to the over-coupling mode, the autodyne signal is inverted. In the case of optimal coupling, when the output power is the highest, the autodyne sensitivity on variation of output power is the lowest and the output response is caused not only by frequency and amplitude variations.

Research results obtained in this paper, calculation relations, and plots of various functions versus values on normalized load and relative amplitude seems to us as useful for engineering parameter and characteristic calculations as well as for determination of optimal operation modes for autodyne microwave oscillators made on the base of Gunn diodes and other active elements.

Acknowledgement

The work was supported by Act 211 Government of the Russian Federation, contract No 02.A03.21.0006.

References

[1] I. V. Komarov and S. M. Smolskiy, *Fundamentals of short-range FM radar*. Norwood, MA: Artech House, 2003. doi: 10.1109/MAES.2004.1346903

[2] A. V. Varavin, A. S. Vasiliev, G. P. Ermak, and I. V. Popov, “Autodyne Gunn-diode transceiver with internal signal detection for short-range linear FM radar sensor,” *Telecomm. Radio Eng.*, vol. 69, no. 5, pp. 451–458, 2010. doi: 10.1615/TelecomRadEng.v69.i5.80

[3] D. A. Usanov and A. E. Postelga, "Reconstruction of Complicated Movement of Part of the Human Body Using Radio Wave Autodyne Signal," *Biomed. Eng. (NY).*, vol. 45, no. 1, pp. 6–8, 2011. doi: 10.1007/s10527-011-9198-9

[4] V. P. Lushev, S. D. Votoropin, Y. N. Deriabin, Y. B. Zharinov, and M. G. Potapov, "Microwave autodyne moving sensors for measurement of burning speed of high-energy composite materials," in *Microwave and Telecommunication Technology (CriMiCo), 2005 15th International Crimean Conference*, 2005, pp. 831–833. (In Russ.). doi: 10.1109/CRMICO.2005.1565160

[5] N. M. Zakarlyuk, V. Y. Noskov, and S. M. Smolskiy, "On-board autodyne velocity sensors for aeroballistics inspections," in *Microwave and Telecommunication Technology (CriMiCo), 2010 20th International Crimean Conference*, 2010, pp. 1065–1068. (In Russ.).

[6] V. Y. Noskov, "A Double-diode autodyne transceiver," *Instruments Exp. Tech.*, vol. 58, no. 3, pp. 505–509, 2015. doi: 10.1134/S0020441215030240

[7] V. Y. Noskov, A. V. Varavin, A. S. Vasiliev, G. P. Ermak, N. M. Zakarlyuk, K. A. Ignatkov, and S. M. Smolskiy, "Modern hybrid-integrated autodyne oscillators of microwave and millimeter wave ranges and their application. Part 9. Autodyne radar applications," *Usp. Sovrem. radioelektroniki*, no. 3, pp. 32–86, 2016. (In Russ.).

[8] K. A. Ignatkov and A. P. Chupahin, "Steady-state mode parameters of the autodyne oscillator," in *Microwave and Telecommunication Technology (CriMiCo), 2015 25th International Crimean Conference*, 2015, pp. 975–976. (In Russ.).

[9] V. Y. Noskov, K. A. Ignatkov, S. M. Smolskiy, and A. P. Chupahin, "Influence of the oscillator operation mode on transfer coefficients of the autodyne response," in *Microwave and Telecommunication Technology (CriMiCo), 2015 25th International Crimean Conference*, 2015, pp. 995–996. (In Russ.).

[10] K. A. Ignatkov, S. M. Smolskiy, and A. P. Chupahin, "Dependence of noise parameters and autodyne characteristics on the oscillator operation mode," in *Microwave and Telecommunication Technology (CriMiCo), 2015 25th International Crimean Conference*, 2015, pp. 997–1000. (In Russ.).

[11] V. Y. Noskov, K. A. Ignatkov, S. M. Smolskiy, and A. P. Chupahin, "Autodyne characteristic dependence upon the oscillator operation mode," in *Microwave and Telecommunication Technology (CriMiCo), 2015 25th International Crimean Conference*, 2015, pp. 992–994. (In Russ.).

[12] V. S. Andreev, "[The influence of the nonlinear properties of the device with negative resistance on the power generated oscillations]," *Radiotehnika*, no. 8, pp. 43–44, 1982. (In Russ.).

[13] I. V. Lebedev, *Tekhnika i pribory SVCh. T. 2. Elektrovakuumnye pribory SVCh*. Moscow: Vysshaya shkola, 1972. (In Russ.).

[14] V. Y. Noskov, K. A. Ignatkov, and S. M. Smolskiy, "Autodyne Characteristic Dependence on the UHF Oscillator's Inherent Parameters," *Radiotekhnika*, no. 6, pp. 24–42, 2012. (In Russ.).

[15] S. D. Votoropin, V. Y. Noskov, and S. M. Smolskiy, "Modern hybrid-integrated autodyne oscillators of microwave and millimeter ranges and their application. Part 2. Theoretical and experimental investigations," *Usp. Sovrem. radioelektroniki*, no. 7, pp. 3–33, 2007. (In Russ.).

[16] V. Y. Noskov and K. A. Ignatkov, "Dynamics of autodyne response formation in microwave generators," *Radioelectron. Commun. Syst.*, vol. 56, no. 5, pp. 227–242, 2013. doi: 10.3103/S0735272713050026

[17] V. Y. Noskov and K. A. Ignatkov, "Dynamic autodyne and modulation characteristics of microwave oscillators," *Telecommun. Radio Eng.*, vol. 72, no. 10, pp. 919–934, 2013. doi: 10.1615/TelecomRadEng.v72.i10.70

[18] V. Y. Noskov and K. A. Ignatkov, “Peculiarities of noise characteristics of autodynes under strong external feedback,” *Russ. Phys. J.*, vol. 56, no. 12, pp. 1445–1460, 2013. doi: 10.1007/s11182-014-0198-6
[19] V. Y. Noskov and G. P. Ermak, “Measurement errors and dynamic range of autodyne vibration meters,” *Telecommun. Radio Eng.*, vol. 73, no. 20, pp. 1843–1861, 2014. doi: 10.1615/TelecomRadEng.v73.i20.50
[20] V. Y. Noskov, “About an energy potential of autodynes,” in *Microwave and Telecommunication Technology (CriMiCo), 2014 24th International Crimean Conference*, 2014, pp. 1029–1030. doi: 10.1109/CRMICO.2014.6959745

Список литературы

1. Komarov I. V., Smolskiy S. M. Fundamentals of short-range FM radar. Norwood: Artech House, 2003. 289 c.
2. Autodyne Gunn-diode transceiver with internal signal detection for short-range linear FM radar sensor / Varavin A. V., Vasiliev A. S., Ermak G. P., Popov I. V. // Telecommunication and Radio Engineering. 2010. Т. 69, № 5. С. 451—458.
3. Усанов Д. А., Постельга А. Э. Восстановление сложного движения участка тела человека по сигналу радиоволнового автодина // Медицинская техника. 2011. Т. 45, № 1. С. 8—10.
4. Автодинные СВЧ датчики перемещения для измерения скорости горения высокоэнергетических композиционных материалов / Лушев В. П., Воторопин С. Д., Дерябин Ю. Н., Журинов Ю. Б., Потапов М. Г. В кн. : 15-я Междунар. Крымская конф. «СВЧ-техника и телекоммуникационные технологии» — КрыМиКо’2005 (Севастополь, 12—16 сент. 2005 г.). 2005. С. 831—833.
5. Закарлюк Н. М., Носков В. Я., Смольский С. М. Бортовые автодинные датчики скорости для аэробаллистических испытаний. В кн. : 20-я Междунар. Крымская конф. «СВЧ-техника и телекоммуникационные технологии» — КрыМиКо’2010 (Севастополь, 13—17 сент. 2010 г.). 2010. С. 1065—1068.
6. Носков В. Я. Двухдиодный автодинный приемопередатчик // Приборы и техника эксперимента. 2015. № 4. С. 65—70.
7. Современные гибридно-интегральные автодинные генераторы микроволнового и миллиметрового диапазонов и их применение. Ч. 9. Радиолокационное применение автодинов /Носков В. Я., Варавин А. В., Васильев А. С., Ермак Г. П., Закарлюк Н. М., Игнатков К. А., Смольский С. М. // Успехи современной радиоэлектроники. 2016. № 3. С. 32—86.
8. Игнатков К. А., Чупахин А. П. Параметры стационарного режима автодинного генератора. В кн. : 25-я Междунар. Крымская конф. «СВЧ-техника и телекоммуникационные технологии» — КрыМиКо’2015 (Севастополь, 6—12 сент. 2015 г.). 2015. С. 975—976.
9. Игнатков К. А., Чупахин А. П. Влияние режима работы генератора на коэффициенты передачи автодинного отклика. В кн. : 25-я Междунар. Крымская конф. «СВЧ-техника и телекоммуникационные технологии» — КрыМиКо’2015 (Севастополь, 6—12 сент. 2015 г.). 2015. С. 995—996.
10. Игнатков К. А., Смольский С. М., Чупахин А. П. Зависимость шумовых параметров и характеристик автодинов от режима работы генератора. В кн. : 25-я Междунар. Крымская конф. «СВЧ-техника и телекоммуникационные технологии» — КрыМиКо’2015 (Севастополь, 6—12 сент. 2015 г.). 2015. С. 997—1000.
11. Носков В. Я. Игнатков К. А., Смольский С. М., Чупахин А. П. Зависимость автодинных характеристик от режима работы генератора. В кн. : 25-я Междунар. Крымская конф. «СВЧ-техника и телекоммуникационные технологии» — КрыМиКо’2015 (Севастополь, 6—12 сент. 2015 г.). 2015. С. 992—994.

12. Андреев В. С. Влияние нелинейных свойств прибора с отрицательным сопротивлением на мощность генерируемых колебаний // Радиотехника. 1982. № 8. С. 43—44.
13. Лебедев И. В. Техника и приборы СВЧ. Т. 2. Электровакуумные приборы СВЧ / Под ред. Н. Д. Девяткова. М. : Высшая школа, 1972. 376 с.
14. Носков В. Я., Игнатков К. А., Смольский С. М. Зависимость автодинных характеристик от внутренних параметров СВЧ генераторов // Радиотехника. 2012. № 6. С. 24—42.
15. Воторопин С. Д., Носков В. Я., Смольский С. М. Современные гибридно-интегральные автодинные генераторы микроволнового и миллиметрового диапазонов и их применение. Часть 2. Теоретические и экспериментальные исследования // Успехи современной радиоэлектроники. 2007. № 7. С. 3—33.
16. Носков В. Я., Игнатков К. А. Динамика формирования автодинного отклика СВЧ генераторов // Известия вузов. Радиоэлектроника. 2013. Т. 56, № 5. С. 21—41.
17. Noskov V. Ya., Ignatkov K. A. Dynamic Autodyne and Modulation Characteristics of Microwave Oscillators // Telecommunication and Radio Engineering. 2013. T. 72, № 10. C. 919—934.
18. Носков В. Я., Игнатков К. А. Особенности шумовых характеристик автодинов при сильной внешней обратной связи // Известия вузов. Физика. 2013. Т. 56, № 12. С. 112—124.
19. Noskov V. Ya., Ermak G. P. Measurement errors and dynamic range of autodyne vibration meters // Telecommunication and Radio Engineering. 2014. T. 73, № 20. C. 1843—1861.
20. Носков В. Я. Об энергетическом потенциале автодинов. В кн. : 24-я Междунар. Крымская конф. «СВЧ-техника и телекоммуникационные технологии» — КрыМиКо’2014 (Севастополь, 7—13 сент. 2014 г.). 2014. С. 1029—1030.

Источники финансирования и выражение признательности

Работа выполнена при финансовой поддержке по постановлению № 211 Правительства Российской Федерации, контракт № 02.A03.21.0006.